DOI: 10.32615/ps.2019.163 PHOTOSYNTHETICA 58 (SI): 379-390, 2020

Special issue in honour of Prof. Reto J. Strasser

Seasonal monitoring of PSII functionality and relative chlorophyll content on a field site in two consecutive years: A case study of different oak species

S. KOLLER[*], V. HOLLAND[**,+], and W. BRÜGGEMANN[*,**]

Biodiversity and Climate Research Centre Frankfurt, Senckenberganlage 25, D-60325 Frankfurt, Germany[*]
Department of Ecology, Evolution and Diversity, Goethe-University Frankfurt, Max-Von-Laue-Straße 13, D-60438 Frankfurt, Germany[**]

Abstract

In search for practical silvicultural management tools to identify alternative tree species for predicted Central European climate conditions, a cross-species survey with five evergreen, semi-evergreen, and deciduous *Quercus* taxa with contrasting morphological leaf traits was performed. Fast chlorophyll fluorescence induction of PSII and relative leaf chlorophyll contents were performed to assess the overall plant vitality at any point in time during two complete vegetation periods in consecutive years (2012 and 2013). Maximum photochemical efficiency of PSII and the performance index on absorption base showed a very conservative relationship to each other and a similar intra-annual progress in all deciduous species, but with a different speed of increase and decrease during leaf development and senescence and thus a different length of vegetation period. The intra-annual variability of OJIP and chlorophyll content parameters is considered with respect to the practicability of measurements in the field for management purposes.

Additional key words: climate change; JIP-test; portable fluorimeter; SPAD.

Introduction

Even for moderate future CO_2 emission scenarios, the Intergovernmental Panel on Climate Change (IPCC) predicts a high probability of a mean annual temperature increase by several degrees in Central Europe, with a higher probability of summer droughts and heat waves for the next century (Schär *et al*. 2004, Christensen *et al*. 2013). These changes could have a large impact on the physiological performance, vulnerability, and productivity of trees in Central Europe. Along with these climatic changes, potential ranges of European tree species are expected to shift (Hickler *et al.* 2012). Less area is suspected to support optimal growth and vitality for beech, spruce, and pine and may be better suited for the more drought-tolerant oaks (Ellenberg 1996). But in some areas of Germany, where native pedunculate (*Quercus robur*) and sessile oak (*Q. petraea*) already represent a large portion of broadleaf tree vegetation, increased vitality losses are noted and expected to increase in the future. In Southern Hesse, the predicted climate change may even provide a potential habitat for Mediterranean oak species (Hanewinkel *et al*. 2013). The seasonal dynamics and species-specific variability of key functional leaf traits for the estimation of plant vitality in oak species of differing natural distributions and adaptations have been monitored under Central European conditions in a common garden type forest experimental plantation in Southern Hesse. Alterations in morphological and pigment leaf traits, changes in the fast chlorophyll (Chl) fluorescence induction transient, and phenological alterations are responses of plants to their environment which occur at different time scales, intensities, and taxa specificity, affecting the potential carbon acquisition capacity of a leaf to different degrees. During leaf development, the leaf is a carbon sink (Thomas and Ougham 2014) and the structure for light capturing is built with species-specific differences in the amount of invested biomass per area of potential light harvest (Wright *et al*. 2004). The concomitant increase in pigments per chloroplast and chloroplasts per cell determine the maximal light-harvesting capacity per time and area (De Pury and Farquhar 1997). On the larger time scale, the potential annual carbon acquisition is furthermore determined by the time of bud break, the end of leaf development, the length of the core vegetation time, the beginning of senescence, and the rate of decline during senescence. At the level of the chloroplast, the

Received 30 August 2019, *accepted* 21 November 2019.
[+]Corresponding author; fax: +49-69-798-42189, e-mail: vholland@gmx.de
Abbreviations: Chl – chlorophyll; doy – day of year; F – fluorescence; M_0 – approximated initial slope of the fluorescence transient; PI_{abs} – performance index on absorption basis; *Q*. – *Quercus*; RC/ABS – Q_A reducing reaction centres per PSII antenna; ϕ_{Po} – maximum photochemical efficiency of PSII; ψ_{Eo} – probability that an electron moves further than Q_A^-.
Acknowledgments: The present study was financially supported by the research funding programme 'LOEWE – The Landes-Offensive in development of scientific and economic excellence in Hesse'.

probability that an absorbed photon leads to the reduction of the primary electron acceptor Q_A can be determined through the ratio of the maximal variable fluorescence to the maximal fluorescence yield (ϕ_{Po}). Further, with the analysis of the OJIP transient and the application of the JIP-test, potential energy losses in the electron transport chain behind PSII can be quantified (Strasser *et al*. 2000, 2004). Decreases in any of the above named, noninvasively measurable photosynthetic leaf traits, are indications for losses in the potential carbon acquisition capacity, and the subsequent steps towards CO_2 fixation involve even more steps of energy loss. Thus, alone or in combination, a monitoring of pigment and photosynthesis traits will provide important supplemental information for the assessment of individual tree vitality at a given time and place. With our study, we provide a reference data set and enable the comparative assessment of key functional photosynthesis-related leaf traits in several European and one American oak species of different functional groups (deciduous, semi-deciduous, evergreen) with a predicted potential range in Central Europe in a changing climate.

Materials and methods

Investigation area: The experimental plantation (~ 0,5 ha) at Frankfurt Schwanheim (50°04'24"N, 08°34'06"E) is situated in the municipal forest of Frankfurt on the Southern Middle Terrace of the Main river valley (95 m a.s.l.) in a ~ 140-year-old *Pinus sylvestris* forest (thinned to 50 trees ha^{-1}). Individual adult trees of *Quercus robur* and *Q. petraea* (80–125 years old) and natural rejuvenations of *Q. robur*, *Q. rubra*, *Rhamnus frangulae*, and *Carpinus betulus* occur at the site. The site is managed for *Rubus fruticosus* agg. and *Calamagrostis epigejos* ground cover. Within the site, a soil profile has been taken and analysed for grain size, soil type, carbon (DIN ISO 10694), and nitrogen content (DIN ISO 13878) by the Hessian Agency for the Environment and Geology (HLUG). Long-term mean annual precipitation sums to 657.8 mm and yearly average temperature was recorded to be 9.7°C (period of 1961–1990, data from German Meteorological Service (DWD), climate station Frankfurt airport, ID 1420). Monitoring wells for ground water depth are located close to the site (G03360, G00620, operated by *Hessenwasser GmbH*). Since 2013, a monitoring well is situated directly on site (HLUG, station ID: 'Schwanheim' 507193). Mean depth of ground water table is given at 3.5 m. In spring 2011, five different *Quercus* species were randomly planted in clusters ('Trupp' scheme) of 21 trees of the same species in 1-m distance to each other (Petersen 2007), resulting in eight clusters each of the following species: *Q. robur* L. (n = 168, 2 years old, provenance: 81707 Upper Rhine Valley, Germany), *Q. pubescens* Willd. (n = 169, 1 year old, provenance: QPU741 Languedoc, France), *Q. frainetto* Ten. (n = 168, 3 years old, provenance: Umbria, Italy), *Q. ilex* L. ssp. *ilex* (n = 168, 1 year old, provenance: QIL701 Sud-Oust, France), and *Q. rubra* L. (n = 168, 2 years old, provenance: 81602), obtained from a tree nursery (*Darmstädter Forstbaumschulen GmbH*). As described in Petersen (2007), a ring of *Carpinus betulus* was added around the clusters (Fig. 1S, *supplement*).

The site was equipped with an on-site climate station (*iMetos sm SMT280*, *Pessl Instruments GmbH*, Weiz, Austria), automatically recording the following parameters in one-hour intervals: air temperature at 2-m height (minimal, maximal, mean) [°C], soil temperature at 20-cm depth (minimal, maximal, mean) [°C], relative humidity [%], dew point temperature [°C], solar radiation [W m^{-2}], precipitation [mm], wind speed [m s^{-1}], and soil water potential at 50-cm depth [cbar].

Seasonal monitoring of Chl content and PSII functionality: The seasonal time course of Chl content and PSII functionality was assessed by monitoring individual leaves of *Q. frainetto*, *Q. ilex*, *Q. pubescens*, *Q. robur*, and *Q. rubra* with the SPAD-meter (*SPAD-502*, *Konica-Minolta*, Osaka, Japan) and records of the fast Chl *a* fluorescence induction transient, measured with the 'plant efficiency analyser' (*Pocket PEA*, *Hansatech*, King's Lynn, UK) in two consecutive years at Frankfurt Schwanheim forest experimental site (Fig. 1S) in 2012 and 2013. Sun-exposed (visually healthy) leaves were labelled at the petiole with a piece of woollen yarn prior to the measurement campaign, shortly after bud break. Since very cold air temperatures in the winter 2011/2012 led to leaf shedding in *Q. ilex*, all monitored leaves in 2012 were leaves developed during that spring. In 2012, monitoring started at 6 June at day of year (doy) 158 and measurements were performed in ~ 2-week intervals (depending on weather conditions) until 8 November (doy 313), resulting in 12 measuring days during the vegetation period 2012. The monitoring of the *Q. ilex* leaves continued in ~ 2-week intervals during the winter period until the start of the 2013 campaign. In 2013, monitoring started at 17 May (doy 137) and ended at 8 November (doy 312), resulting in 13 measuring days in ~ 2-week intervals during the vegetation period 2013. For the monitoring campaign 2013, the same trees as in 2012 were monitored again. In *Q. ilex*, additionally to the leaves monitored in 2012, current year leaves of 2013 were added to the monitoring program. To ensure comparability of Chl *a* fluorescence data, all *PEA* measurements were performed at night between midnight and day break. SPAD measurements were usually performed at early morning after sunrise. To cover possible spatial variability, three trees per cluster were selected, resulting in 24 leaves per species distributed over the plantation and 120 leaves per measuring day in 2012 (144 in 2013). One fast Chl *a* fluorescence transient was recorded per leaf, whereas for the SPAD values, the mean of five measurements per leaf was documented.

The time course of Chl content comprises an increase in spring, followed by a period with minimal change and a decline in autumn. The equations of three linear regressions, individually fitted to the data points of each leaf, were used to derive the rate of increase at the phase of spring development and the rate of decline at autumnal senescence from the slopes of the regressions. The intersections of the linear regressions were used to quantify the end of development and the beginning of senescence, as well as to calculate the 'core vegetation

time'. Full data sets for the whole vegetation period were available for 2013; in 2012, spring measurements started on doy 158, so the initial leaf development phase was not covered. The mean, the maximum and standard deviation (SD) of all SPAD values within the core vegetation time were also calculated for each individual leaf. The relative SPAD values were also calculated for every individual leaf with $SPAD_{rel} = SPAD_i \times SPAD_{core}^{-1} \times 100$, where $SPAD_i$ is the individual SPAD value at the time i and $SPAD_{core}$ is the mean SPAD value in the period of core vegetation time. The parameter estimations were carried out in *Microsoft Excel* (*version 2010*) for leaves with complete traces.

For the analysis of the fast Chl *a* fluorescence transient, parameters were calculated with the provided *PEA Plus* software (*Hansatech*, *version 1.02*) with the F_0 level set to 50 µs and the *Biolyzer* software (*version 3.0*, Ronald M. Rodriguez, Bioenergetics Lab. Geneva, Switzerland). Parameters were calculated according to Strasser and Strasser (1995) and Strasser *et al.* (2000, 2004). For the seasonal time course analysis, the maximum quantum yield of primary photochemistry: ϕ_{Po} [$= F_v/F_m = (F_m - F_0)\ F_m^{-1}$] and the logarithmised performance index on absorption basis ($lnPI_{abs}$, Strasser *et al.* 2000) were calculated (Appendix). To assess possible differences in the shape of the Chl *a* transients at different days of the year, original Chl *a* transient data were additionally normalised to F_0 ($= F_{50\mu s}$) for equal starting points, double normalised to F_0 and F_m (V_{OP}) to rank all fluorescence values between zero and 1 or further calculated as differential V_{OP} curves (ΔV_{OP}) as depicted in Appendix.

Statistical analysis: Data import and management was conducted with *Microsoft Excel* (*version 2010*, Redmond, Washington, USA). Following a one-way analysis of variance (*ANOVA*) with *Tukey*'s post-test for multiple comparison was performed and models were fit to the data with *GraphPad Prism*'s (*version 5.04*, La Jolla, USA) linear and nonlinear regression equations. The homographic model was added manually to the software. Coefficients of correlation (*Pearson*'s *r*) and determination (R^2), model comparisons and best fit parameter estimations were calculated by the statistical software as well.

Results

Climate at Frankfurt Schwanheim in 2012 and 2013: The climate conditions of 2012 and 2013 at the site are outlined at daily resolution (Fig. 1). A significant temperature drop at the end of January marked the beginning of 2012 with minimum air temperature of –17.1°C. This period of low temperature in early 2012 led to total leaf shedding in *Q. ilex*. Frost events were frequent until the end of April 2012, with a following sharp increase in air temperature to over 30°C at the end of April. Late frost occurred in the middle of May. The highest temperature recorded in 2012 was 36.1°C at the end of August, when (in combination with a period of low precipitation) a soil water deficit developed, which peaked in September (Fig. 1). The duration of soil water potentials below –200 cbar (limit of watermark sensor) cannot be given, since the functionality of the sensor was lost due to the dry conditions. After a warm December, temperatures plummeted in January 2013 with icy rain, leading to ice crusts on leaves. The beginning of the year 2013 was colder compared to 2012 with mean daily temperatures around zero to 5°C until the middle of April. The lowest temperature was recorded in March with –12.3°C. A late frost occurred at the end of May. In the end of July, a period of hot days occurred with a maximum temperature of 37.4°C. Simultaneously a soil water deficit developed from the beginning of June and reached –200 cbar in 1-m depth at the beginning of August, declining in September.

Chlorophyll content and PSII functionality: From the time course of SPAD values in the growth period, three distinct periods were identified (Fig. 2). At the beginning of the growth period, SPAD values increased until a plateau was reached. Variations at the plateau were small and fall within the range of leaf scale variability. At a time point, which marked the individual beginning of senescence, SPAD values dropped until the leaf abscised.

In 2013, SPAD values increased at a rate of approx. 3 to 5 SPAD units per week. *Q. rubra* showed the slowest rate of increase with 3.0 ± 0.9 per week, which differed significantly from the other *Quercus* species (*Q. frainetto*:

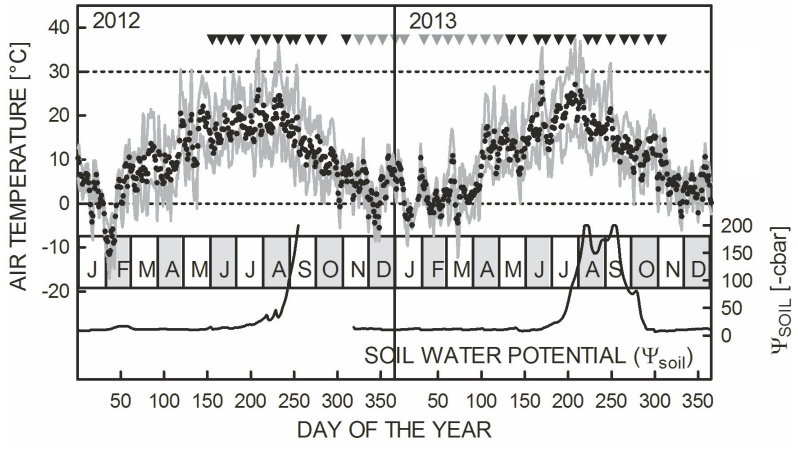

Fig. 1. Temperature and soil water deficit at Frankfurt Schwanheim in 2012 and 2013. Daily minimum and maximum temperatures are indicated in greyscale above and below mean daily temperature (*black dots*) measured at 2 m height. *Horizontal broken lines* indicate 0 and 30°C. Soil water potential in (–)cbar (0–200) measured at 1 m depth on right *y*-axis. Values from September to November 2012 are missing. Months are indicated by alternate *grey* and *white boxes* in the bottom third of the graph. *Triangles* symbolize days of SPAD and predawn OJIP measurements of *Quercus frainetto*, *Q. robur*, *Q. pubescens*, *Q. rubra*, and *Q. ilex*. Winter measurements symbolized by *grey triangles* only for *Q. ilex*.

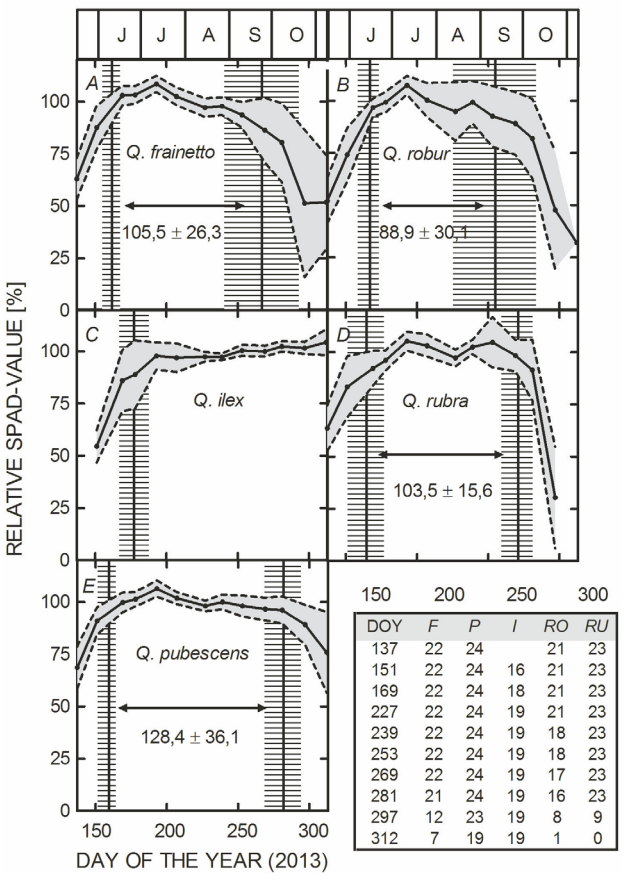

Fig. 2. Seasonal variability of SPAD readings and derived developmental parameters for 2013 at Frankfurt Schwanheim. Rel. SPAD values [%] of *Quercus frainetto* (*A*), *Q. robur* (*B*), *Q. ilex* (*C*), *Q. rubra* (*D*), and *Q. pubescens* (*E*). Sample sizes table on the bottom right (doy 178, 193, and 207 not shown). Rel. SPAD values (*black line*) calculated for every individual leaf. *Broken line* and *the grey shading*: Standard deviations. *Vertical solid lines* represent the end of development and beginning of senescence. SDs indicated by *stacked horizontal lines*. Mean and SD of the core vegetation time are displayed in the graph's centre. Since the evergreen *Q. ilex* shows no senescence, the core vegetation time cannot be calculated.

4.8 ± 1.1; *Q. ilex*: 5.5 ± 1.4; *Q. pubescens*: 4.1 ± 1.4; *Q. robur*: 4.1 ± 1.0; Table 1S, *supplement*). All deciduous species reached the plateau in the middle of June. No significant interspecific difference for this time point could be observed for the deciduous species. *Q. ilex* reached the plateau as the last species between the end of June and the beginning of July, but earlier than the end of structural leaf development (morphological data not shown). Since there was no significant difference in the time when the plateau was reached, the duration of the plateau phase correlated with the beginning of senescence ($R^2 = 0.841$) in 2013. *Q. frainetto* and *Q. robur* showed large intraspecific variation for the beginning of senescence (SD 26–30 d). In senescing leaves, the slowest rate of decrease was observed in *Q. pubescens* resulting in 80% of leaves still being measurable at doy 312, whereas in *Q. rubra* only one of initially 24 leaves was left at doy 312 and 60% were already abscised two weeks prior. The SD of the mean SPAD value at the core vegetation time was generally low in a range from 1.6 (*Q. ilex*, *Q. pubescens*) to 2.4 (*Q. frainetto*) and within the range of standard deviations measured at the leaf scale. Alterations and fluctuations of SPAD values during the year were low and no trend of possible reaction to an abiotic factor was observed other than the development of the leaves and the beginning of senescence.

In *Q. ilex* autumnal senescence did not occur and a slight trend towards higher SPAD values to the end of the year was observed. Additionally, a large intraspecific variance was noted in *Q. ilex* early in the growth period, when some leaves reached plateau values, while others were still 25% below these values. Differences between the species were apparent later in the growth period. In *Q. pubescens*, senescence started late and the decline was rather low. Hence, 19 of initially 24 leaves were still measurable at doy 312 and the mean was not lower than 75% of the plateau phase value. *Q. pubescens* showed the longest core vegetation time of all studied deciduous species and was the only species (besides the *Q. ilex*) with all values of $SPAD_{rel}$ above 50% at the beginning of November (Fig. 2). In contrast to *Q. pubescens*, *Q. rubra* showed a rather collective beginning of senescence with a rapid decline: within a period of 16 d, 60% of all measured leaves were abscised or no data could be recorded. Fifteen days later, not a single leaf was measurable. In *Q. frainetto* and *Q. robur*, the intraspecific variability in the beginning of senescence was marked by high SDs. Single leaves showed declining values at the end of August, while other leaves showed no signs of Chl decline until the beginning of October. Lab analysis of the absolute contents of Chl *a* and Chl *b* were nonlinearly correlated to SPAD readings (Fig. 3S*F*, *supplement*) with high R^2 (Chl *a*: 0.903; Chl *b*: 0.832; $n = 490$), prompting us to use the SPAD readings for further correlation analysis. No correlation was found between the mean SPAD value at core vegetation time and the beginning of senescence. PSII functionality was assessed by parameters derived from predawn fluorescence measurements of the fast OJIP fluorescence transient. Overall PSII functionality was estimated by the maximum quantum yield of PSII (ϕ_{Po}) and the performance index (PI_{abs}). A seasonal trend, similar to the seasonal time course of relative Chl content was observed for ϕ_{Po} and PI_{abs} in 2012 and 2013 (Fig. 3). A parameter rise at the time of leaf development led to a period with little change of parameter amplitude, followed by a substantial decrease at the end of the growing season (except for the evergreen *Q. ilex*). First measured ϕ_{Po} values at doy 137 (17 May 2013), early after bud break, were above 0.6 in all species. After the initial increase, ϕ_{Po} values showed little alteration and were in a range of 0.81 to 0.82 in 2012 (median for doy 180–248) and 0.79 to 0.81 in 2013 (median for doy 178–269). The time course of PI_{abs} (transformed by natural logarithm) resembled the time course of ϕ_{Po} in most parts and noticeable deviations in ϕ_{Po} were seen intensified in $\ln PI_{abs}$. In the autumnal decrease the values of ϕ_{Po} and $\ln PI_{abs}$ remained artificially high, since sample sizes decreased from the beginning of

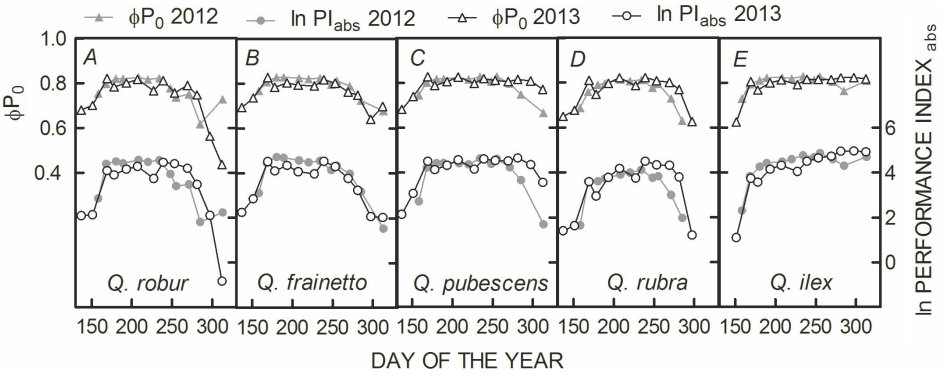

Fig. 3. Seasonal variability of the maximum quantum yield of primary photochemistry of PSII (ϕ_{Po}) and the logarithmised performance index on absorption basis ($lnPI_{abs}$) in 2012 and 2013 at Frankfurt Schwanheim. Parameter means of ϕ_{Po} (*upper curves*) and $lnPI_{abs}$ (*lower curves*) of *Quercus robur* (*A*) *Q. frainetto* (*B*), *Q. pubescens* (*C*), *Q. rubra* (*D*), and *Q. ilex* (*E*) in 2012 (*grey line*) and 2013 (*black line*).

October by leaf abscission (Fig. 3) and data from leaves far progressed in senescence (not measureable) could not be obtained. Early increase and development of the ϕ_{Po} and $lnPI_{abs}$ showed little inter-annual variability, while the period of higher PSII functionality seemed to be longer in 2013 compared to 2012 in *Q. pubescens*, *Q. robur*, and *Q. rubra*. In *Q. frainetto*, the decrease of ϕ_{Po} and $lnPI_{abs}$ did not vary between 2012 and 2013. In *Q. ilex*, both parameters showed no tendency of decrease towards the end of the growing season and $lnPI_{abs}$ seemed to further increase with time in 2013. Also in 2013, in all species a small depression after the initial increase was noted in ϕ_{Po} and $lnPI_{abs}$ alike, at the fourth measurement in 2013 (doy 178; 27 June 2013). A second local minimum in both parameters was observed during the summer at doy 227 (15 August 2013) which is more pronounced in $lnPI_{abs}$ than in ϕ_{Po}. In 2012, only one depression at the beginning of the growth period was observed at doy180 (28 June 2012) in $lnPI_{abs}$ in *Q. robur* and *Q. rubra*.

To quantify inter-annual and interspecific differences of PSII functionality for distinct periods of time, the area below the individual leaf time courses of $lnPI_{abs}$ was calculated (data not shown). For the whole growing season, *Q. ilex* showed the highest values, despite of delayed development, since PSII functionality was not decreasing at the end of the year. Due to delayed senescence (especially in 2013), *Q. pubescens* showed high values as well.

When transients were normalized to F_0 (for equal starting intensities), F_J, F_I, and F_m decreased (less difference in F_J) at early measuring dates during leaf development compared to later measuring dates (Fig. 4*A*). However, the fluorescence yield increase at different times was disproportional, resulting in an increased J-step at 2 ms at doy 137 and doy 151, when the transient was normalized to F_0 and F_m (Fig. 4*B*). This difference was further visualized by subtracting the transients obtained on doy 207 (completed leaf development), by which two local maxima became apparent close to the J-step (Fig. 4*C*). The largest peaks at the J-step occurred at the earliest measuring date (doy 137). The signal was reduced two weeks later, but still clearly identifiable at doy 151. At the I-step (30 ms), neither in V_{OP} transients, nor in the differential curves, differences were noted (Fig. *4B*,*C*) despite of lower F_I intensities (Fig. 4*A*). During autumnal senescence, a reversed trend was observed and fluorescence intensities (again most noticeable at F_I and

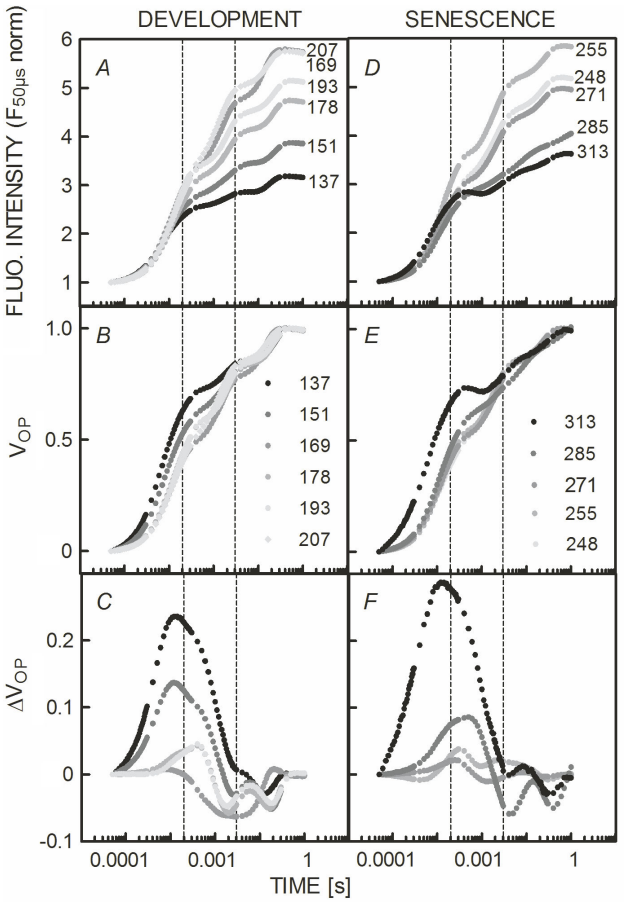

Fig. 4. Fluorescence transient alterations during leaf development and senescence. Mean transients of *Quercus pubescens* are shown (n = 19–24), measured predawn at given day of the year (Development: 2013; Senescence: 2012). (*A*,*E*) Fluorescence intensity normalized to $F_{50\mu s}$. (*B*,*E*) Double normalized transients $V_{OP} = (F_t - F_0)(F_m - F_0)^{-1}$. (*C*,*E*) Differential V_{OP} curves. Development: $\Delta V_{OP} = V_{OPdoyi} - V_{OPdoy207}$; Senescence: $\Delta V_{OP} = V_{OPdoyi} - V_{OPdoy248}$. *Vertical broken lines* indicate J- (2 ms) and I-step (30 ms) of the OJIP transient. Note logarithmical *x*-axis.

F_m) decreased as autumn progressed (Fig. 4*D*). The V_{OP} transients showed a deviation from the typical OJIP shape at doy 285 with increased fluorescence at the J-step and a decreased I-step. At doy 313, fluorescence at the J-step strongly increased, showing a local maximum instead

of the usual plateau. Further, the slope to the J-step was markedly intensified (Fig. 4*E*). In the differential curves, a large peak very close to the J-level was observed for doy 313 and a minor peak at doy 285. At the I-level, no increase compared to the earlier measuring dates was noted (Fig. 4*F*). Comparing the fluorescence kinetics of leaf development and leaf senescence, similarities were apparent: in both cases the total fluorescence decreased, yet disproportionally, leading to relative increases around 2 ms. At the seasonal time course of PSII functionality (Fig. 3), the comparably lower fluorescence intensities at F_m early and late in growing season led to the decreased maximum quantum yield of primary photochemistry (ϕ_{Po}). The inclusion of the relative fluorescence intensity at the J-step in the calculation of PI_{abs} led to stronger increases during leaf development and greater decreases during leaf senescence compared to ϕ_{Po}.

Relationship between JIP-test parameters: All selected JIP-test parameters were significantly related, following distinct associations (Fig. 5). The two parameters most often used to describe the functionality of primary photochemistry, ϕ_{Po} and PI_{abs}, showed a very conservative relationship. Higher PI_{abs} values than 3 were only observed at ϕ_{Po} above 0.7. Leaves with ϕ_{Po} values below 0.7 were always correlated with very low values of PI_{abs}, but at ϕ_{Po} values above 0.7, the whole range of PI_{abs} values could be observed (Fig. 5*A*). The relationship of ϕ_{Po} to RC/ABS, quantifying Q_A reducing RCs per PSII antenna Chl, was similar to the relationship of ϕ_{Po} to PI_{abs}, with a linear decline of ϕ_{Po} at RC/ABS threshold of 0.5 (Fig. 5*C*). PI_{abs} consists of three components [RC/ABS, $\psi_{Eo}/(1 - \psi_{Eo})$, and $\phi_{Po}/(1 - \phi_{Po})$; Appendix], of which the one with the greatest range of values is $\phi_{Po}/(1 - \phi_{Po})$. Whereas the relationship of PI_{abs} to RC/ABS appeared nonlinear (Fig. 5*B*), the relationship of PI_{abs} to $\psi_{Eo}/(1 - \psi_{Eo})$ showed a linear development at increasing $\psi_{Eo}/(1 - \psi_{Eo})$ values beyond 1 (Fig. 5*D*), indicating a difference in the influence of component changes to PI_{abs}. $V_{OJ300\mu s}$, a parameter quantifying the K-step, indicative for limitations at the electron donor side of PSII, was found to only increase significantly at extremely low PI_{abs} values (Fig. 5*E*).

Relationship between SPAD readings and JIP-test parameters: The measurements of SPAD and JIP-test values were performed on the same leaves; therefore it was possible to directly correlate the parameters with each other. No interspecific differences in the correlations were found. Fig. 6*A*,*B* shows the positive correlations of SPAD values with absolute fluorescence intensities. F_m was linearly correlated over the whole range with the SPAD readings. For F_0, after an initial increase at SPAD values of approx. 20 to 25, a decreasing slope was noted. Fig. 6*C*,*D* shows the correlations for the normalized fluorescence parameters of the J- (2 ms) and I- (30 ms) step: V_J and V_I [$V_t = (F_t - F_0)/(F_m - F_0)$]. For both parameters, negative linear relationships to the SPAD values, with a difference in parameter range, and therefore a difference in slope were observed. RC/ABS, which is calculated including the approximated initial slope of the fluorescence transient [$M_0 = 4(F_{300\mu s} - F_{50\mu s})/(F_m - F_{50\mu s})$; Appendix], V_J and ϕ_{Po}, is one of three terms, expressing partial potentials at steps of energy bifurcations [$PI_{abs} = RC/ABS \times \psi_{Eo}/(1 - \psi_{Eo}) \times \phi_{Po}/(1 - \phi_{Po})$, definition by Strasser *et al.* 2010]. The correlation of PI_{abs} to SPAD values was different to the correlations mentioned before. SPAD values above 30 could be associated with high or low values of PI_{abs}, whereas at low SPAD values, no high values of PI_{abs} were observed.

Discussion

Seasonal monitoring of Chl content and PSII functionality: The Chl content, as an estimator of the plant's light-harvesting capacity and the fluorescence parameters, ϕ_{Po} and PI_{abs}, used for the estimation of the quantum yield of primary photochemistry and energy conservation to the reduction of the intersystem electron acceptors, followed

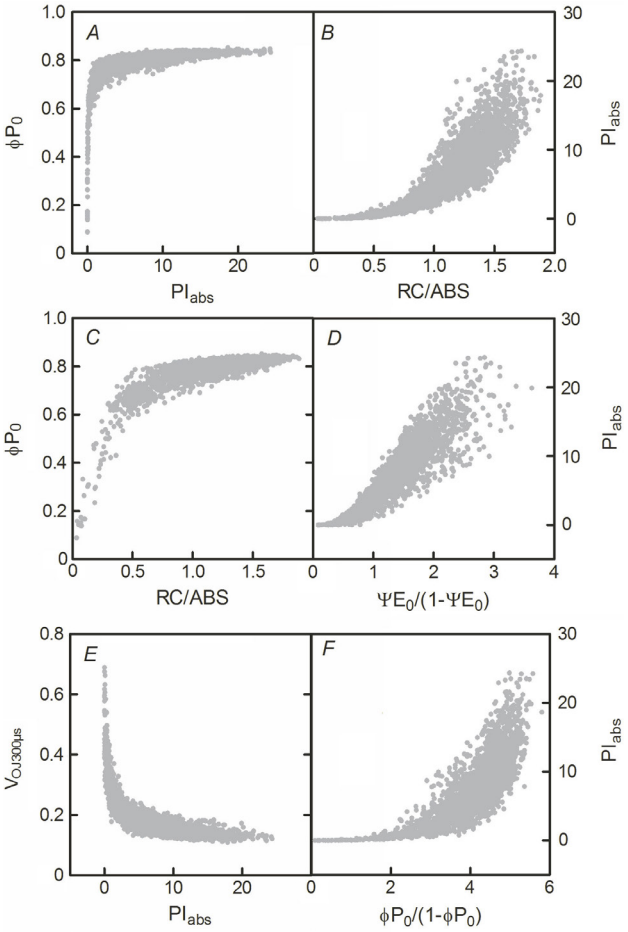

Fig. 5. Relationship between JIP-test parameters during leaf development, senescence, and steady state: maximum quantum yield of the primary photochemistry of PSII (ϕ_{Po}), performance index on absorption basis (PI_{abs}), relative amplitude of the K-step ($V_{OJ300\mu s}$),efficiency that the an electron moves further than Q_A^- (ψ_{Eo}), Q_A-reducing reaction centre per PSII antenna (RC/ABS). Number of independent data points = 2527. Species: *Quercus frainetto*, *Q. ilex* (current and previous year leaves), *Q. robur*, and *Q. rubra* in 2012 and 2013. Day of year range 137–313.

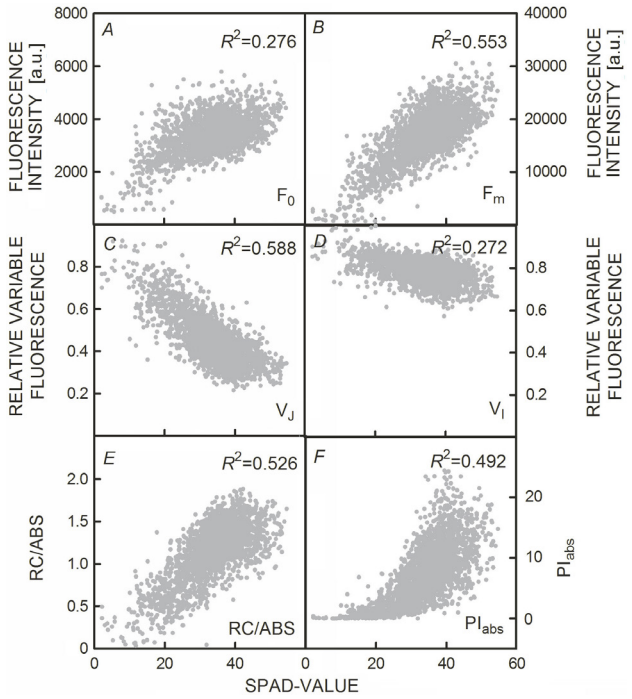

Fig. 6. Correlations between SPAD values and JIP-test parameters. (*A–F*) show independent data points of *Quercus frainetto*, *Q. ilex* (current year leaves), *Q. pubescens*, *Q. robur,* and *Q. rubra* from 2012 and 2013, including dates with leaf development and senescence (n = 2522). (*A*) minimal fluorescence; (*B*) maximal fluorescence; (*C*) relative variable fluorescence at J-step (2 ms); (*D*) relative variable fluorescence at I-step (30 ms); (*E*) Q_A-reducing reaction centres per PSII antenna chlorophyll; (*F*) performance index for energy conservation from photons absorbed by PSII to the reduction of intersystem electron acceptors. All parameters are significantly correlated with SPAD values (P<0.0001; *Pearson*'s r test for correlation).

three distinct stages during the growth period in all investigated species: a rise in the spring during leaf development, a steady-state phase with little change, and a subsequent decline in late summer and autumn (except in the evergreen *Q. ilex*, for which no decline was observed; Figs. 2, 3). It has to be considered that the seasonal monitoring of Chl contents and Chl fluorescence refers to the first flush only. Since leaf growth in *Quercus* is episodic, a second flush (or even a third) may occur during the season, from which the described phases and rates may differ.

The time of bud break of the first flush is sensitive to the nonvariable photoperiod (Körner and Basler 2010), but shows a certain amount of plasticity, influenced by variable factors such as temperature in winter and spring (Bussotti *et al*. 2015). It is further genetically controlled and differs between *Quercus* provenances planted on the same site (Bussotti *et al.* 2015); trees of provenances with climates, in which phenological tracking of temperatures bears a smaller risk of injury, might be less sensitive to the photoperiod and thus more likely to track temperature changes in spring (Körner and Basler 2010). *Q. robur* is considered a late leafing species (Sparks and Carey 1995) but the other investigated *Quercus* species did not significantly differ in the timing of bud break from *Q. robur* at the site (except for *Q. ilex*). For South England, Morecroft *et al*. (2003) reported bud break for *Q. robur* between mid-April and the beginning of May (doy 102–121; 1996, 1999, 2000). In southern Hesse, Both and Brüggemann (2009) observed bud break in solitary and mature *Q. robur* at doy 110 and 123 (2006, 2007). A warming climate with increased spring-time temperatures could promote earlier bud break (Körner and Basler 2010, Kovats *et al*. 2014). Phenological records since 1950 show a tendency for increasingly earlier leaf development in *Q. robur* (0.12 d per year: 1951–1996; Menzel 2003), especially during the last two decades (Schleip *et al.* 2011). Earlier bud break may provide a competitive advantage, primarily because light intensity and day length peak at late June and decrease subsequently leading to similarly decreasing daily potential photosynthetic carbon uptakes (Morecroft *et al*. 2003). On the other hand, late frost events like in May 2011 (locally to –10°C; Fig. 2S, *supplement*) pose a serious threat to the developing tissue and lead to damage or even total loss of the flush, resetting spring development by 7–9 weeks (Kreyling *et al.* 2012). *Q. ilex* can make use of favourable conditions in early spring with its previous year leaves, which are not susceptible to late frost (*i.e*., above –20°C). Bud break often occurs later than in the deciduous species as observed in 2013 (Both and Brüggemann 2009); delayed by 20 d compared to *Q. robur*, thus avoiding late frost damage on immature leaf tissue.

Leaf development after bud break in spring as well as the previously occurring stem growth (~ 10 d before bud break; Barbaroux and Bréda 2002), rely entirely on surplus reserves, stored during the previous year growing season (Lacointe *et al*. 1993, Barbaroux and Bréda 2002) until a positive carbon balance is reached in the developing leaves (~ 11 d in *Q. robur*; Morecroft *et al*. 2003). Leaf expansion is relatively fast (~ 15 d from bud break to maximal leaf area in *Q. petraea*; Barbaroux and Bréda 2002) and less variable than the speed of leaf maturation (Miyazawa *et al*. 1998). The rate of photosynthesis at saturating light intensity increases during leaf development and it has been found to reach full capacity with the completion of the structural development (Miyazawa *et al*. 1998), which was attained by mid-June in all deciduous species (data not shown). Morecroft *et al*. (2003) reported a period of up to 70 d for photosynthetic maturation in *Q. robur* in England, whereas a period of only 30 d was reported under Mediterranean climate conditions by Grassi and Magnani (2005). Despite of the slow attainment of full photosynthetic capacity, the light-harvesting capacity and electron supply to the Calvin cycle were fully sufficient 7 d after bud break, with ϕ_{Po} values > 0.7 (Both and Brüggemann 2009). Nevertheless, energy supply exceeded the capacity of energy use by photosynthesis and their capacity for energy dissipation during the day, leading to photoinhibition and decreased midday ϕ_{Po} values of < 0.4 one week after bud break. The slow development of full photosynthetic capacity despite of already sufficient light-harvesting capacity was assumed to be related to a

low carbon sink strength in spring (Both and Brüggemann 2009), which on the other hand can be influenced by climate (Bauerle *et al*. 2012). In the present study, ϕ_{Po} did not increase significantly faster than the morphological leaf traits or Chl contents in the deciduous species, but predawn ϕ_{Po} values were already above 0.6 in all species at the first time date of measurement in 2013 (doy 137). In *Q ilex*, ϕ_{Po} values reached optimal levels (0.76–0.83) earlier than structural maturation and the end of development. As stated above, an earlier bud break and faster photosynthetic leaf maturation have a more pronounced effect on the potential photosynthetic carbon gain due to increased day length and light intensity than delayed senescence begin in autumn. The potential maximum light-harvesting capacity can be sensed and quantified by the Chl content and the recording of the fast Chl *a* fluorescence transient, but light harvesting and PSII integrity are not the only limiting factors for photosynthetic productivity in spring as Both and Brüggemann (2009) have pointed out. Analysis of the fast Chl *a* induction curves reveal a similar fluorescence O-J rise with steadily increasing intensity of maximal fluorescence yield in developing leaves (Fig. 3) of all species alike. The photochemical phase (O-J rise), related mainly to the reduction of the primary electron acceptor Q_A and strongly dependent on the number of absorbed photons (Stirbet and Govindjee 2012), was less affected by leaf age than the thermal phase (J-I-P rise, Stirbet and Govindjee 2012). This led to differences in the time resolved double normalized fluorescence yields. The differential V_{OP} curves (ΔV_{OP}) showed a peak at around 1 ms at the first date of measurement (Fig. 3*C*), which steadily declined and transitioned to a smaller shoulder at ~ 9 ms as leaves got older. The shapes of the OJIP transients and their change of shape with time during leaf development were very similar to the transients developing during autumnal leaf senescence (Fig. 3*F*). Holland *et al*. (2014) observed similar changes in OJIP transients during natural autumnal senescence of different deciduous *Quercus* taxa. The peak at the J-level (~ 2 ms) is associated with a decrease of Q_A^- reoxidation, since the disablement of Q_A^- reoxidation results in maximal fluorescence yield (F_m) at the J-step without influencing the O-J rise (Kalaji *et al.* 2014). A decrease in the rate of Q_A^- reoxidation can be due to a decreased PQ pool size and/or a reduction of electron transport acceptors in and around PSI (Schansker *et al.* 2005, Kalaji *et al.* 2014). Thus trapped energy is disposed effectively at an early step in the electron transport chain, decreasing the risk of a high electron pressure at times of low photosynthetic capacity. It seems as if not energy absorption, but energy trapping and electron transport are the limiting factors during both photosynthetic leaf maturation and senescence. A difference in the rate of development of the potential light-harvesting capacity by increased rate of Chl accumulation does not by itself seem to translate into a competitive advantage of trees or species. Since PI_{abs} is calculated as a function of three components (RC/ABS, ψ_{Eo}, ϕ_{Po}), which represent important steps of energy bifurcations, limitations in energy trapping and electron transport translate into decreased PI_{abs} values (even when the maximum quantum yield is quite stable over a wide range of PI_{abs}; Fig. 5*A*) and may thus be preferred to quantify the performance capacity of PSII. Based on the range of possible approachable values of the three components of PI_{abs}, alteration at different steps of the OJIP transient influence PI_{abs} to a different degree (*cf.* Fig. 5*B*,*D*,*F*). It must be noted, however, that (at least under natural conditions) changes in PI_{abs} are the result of alterations in all components at the same time. Additional to the fluorescence intensities at O- and the P-step [F_0 and F_m; $(F_m - F_0)/F_m = \phi_{Po}$)] changes at the K- ($F_{300\mu s}$) and the J-step ($F_{2ms}$) have an impact on PI_{abs}. $F_{300\mu s}$ is used in the calculation of RC/ABS only, whereas F_{2ms} is used in the calculation of RC/ABS and ψ_{Eo}. Changes in ϕ_{Po} showed the largest influence on PI_{abs}, since the parameter is an element in the calculation of all three components. In the relationship of the JIP-test parameters to each other, certain threshold values were apparent, beyond which PSII functionality appeared to be severely suppressed. At RC/ABS values below 1, only very low PI_{abs} values were observed, whereas gradual decreases of ϕ_{Po} were noted at RC/ABS values below 0.5. In leaf samples with very low PI_{abs} values (recorded primarily during leaf senescence), $V_{OJ300\mu s}$ revealed a strong increase (Fig. 5*E*). $V_{OJ300\mu s}$ quantifies the K-step in the altered OJIP transient (to OKJIP; Guissé *et al*. 1995), associated with the impairment of electron donation by the oxygen-evolving complex (Srivastava *et al*. 1997, Strasser 1997, Oukarroum *et al*. 2007).

The steady-state phase, defined as the time interval in the vegetation period when the influence of leaf development and leaf senescence were insignificant (termed 'core vegetation time'), was characterized by more or less constant values with low variability. In the steady-state phase, the fluorescence parameters showed no interspecific variability. The maximum quantum yield of primary photochemistry (ϕ_{Po}) was in a range of values described for healthy samples (Björkmann and Demmig 1987, Mohammed *et al.* 2003), indicating daytime conditions did not lead to prolonged photoinhibition. In contrast to the fluorescence parameters ϕ_{Po} and $\ln PI_{abs}$, Chl contents, measured as SPAD values, varied between species in the steady-state phase (Fig. 2, Table 1S). The Chl contents variability during this stage was low for individual leaves (1.6–2.4 SD). Trees with lower Chl contents in 2012 also showed lower values in 2013 and *vice versa* (data not shown), indicating that factors influence the leaf greenness on small spatial scales. Additionally, SPAD values of different leaves on a single tree did not vary to a large extent. The length of the core vegetation time was correlated to the onset of senescence in 2013 (not shown), due to similar time points for the end of the leaf development phase (Table 1S), which may have been influenced by very low spring-time temperatures in this particular year, synchronizing bud break of the different species. On a larger time scale (1951–1996), the growing season for *Q. robur* in Germany showed an increasing trend of 0.22 d per year due to earlier bud break and later begin of senescence (Menzel 2003), and expected further changes in phenology are highly confident in climate change scenarios (Kovats *et al*. 2014). Photosynthesis

is primarily influenced by the absorbed irradiance, the biochemical capacity for photosynthesis (rate of carboxylation and rate of electron transport), temperature, and the CO_2 concentration at the carboxylation site (De Pury and Farquhar 1997). An increased amount of Chl per unit area would lead to a higher amount of absorbed irradiance per growing season (De Pury and Farquhar 1997). In this context, trees displaying high SPAD values during the growing season with inter-annual continuity, would benefit from a higher annual carbon acquisition, which could lead to an additional flush, further increasing leaf area and height, increasing root growth or increasing nonstructural carbon reserves, resulting in a an advantage over its competitors. Despite of less favourable conditions for photosynthesis and carbon gain in the late growing season (Morecroft *et al*. 2003), a delay or deceleration of the senescence process may provide a competitive advantage, since it results in prolonged storage of reservoir carbohydrates and root growth (Larcher 1994). The senescence process is generally assumed to be comprised of several phases. In a first phase, total Chl, nitrogen, and protein contents decrease in a balanced matter (Munné-Bosch and Alegre 2004), not affecting the quantum yield efficiency of primary photochemistry (Miersch *et al*. 2000). In a second phase, the senescence process is accompanied by further decrease in Chl content with impairments of the photosynthetic electron transport and changing Chl *a*/*b* ratios (Holland *et al.* 2014). Senescence can be affected by water and nitrogen availability, temperature or photoperiod (Addicott 1968, Larcher 2003, Munné-Bosch and Alegre 2004, Estrella and Menzel 2006, Delpierre *et al.* 2009, Balazadeh *et al.* 2014). A good correlation was found between the beginning of senescence and the duration of the core vegetation time in 2013 (not shown), since leaf development was very similar in all deciduous trees and species in this particular year. A soil water deficit developed in both years (Fig. 1), apparently by decreasing values of soil water potential, but at different times of the year. In 2012, soil water deficit developed in the beginning of August and reached the –200 cbar mark at mid-September, leading to an earlier (but not significant) beginning of senescence, as compared to 2013. In 2013, water deficit developed in July and reached the –200 cbar mark at the beginning of August, which presumably resulted in a later onset of senescence, however, the rate of Chl decrease was faster. *Q. rubra* seemed to be most affected by the decreased soil water potential. Abrams (1990) reported that *Q. rubra* was more restricted to mesic sites, representing an exception of North American oaks, which mostly are considered to be relatively drought resistant. Contrary to the senescence behaviour of the other deciduous species, *Q. pubescens* showed no alteration in the beginning of senescence or in the rate of decrease between both years, so that only a very small number of leaves were abscised and the Chl content of remaining leaves was still high at the last day of measurement in November 2013. The increased period of leaf greenness and the sustained high values of maximal quantum yield resulted in an increased period of light harvesting and potential carbon gain compared to the other deciduous species. Since *Q. pubescens* trees did not show a higher number of leaf flushes per year as compared to *Q. robur* and similar aboveground height, the carbon surplus assimilated during the prolonged vegetation period may provide increased root growth, favourable for stands with low soil moisture and nutrient contents. *Q. ilex* with a true evergreen leaf life strategy can benefit from warm autumnal and early winter temperatures.

The information about the annual time course of leaf Chl content and quantum yield efficiency is of great importance when representative values for a comparative analysis between different species in the same developmental stage or different years have to be estimated. Otherwise developmental stages may mask or blur the observed effect of a stressor. Since the developmental phase and the beginning of senescence may vary between species, the time period of the core vegetation time seems most appropriate for this task. During this phase, changes in SPAD values were small (mean SD = 1.9). Based on the observations in 2012 and 2013, the period from mid of July to mid of August would yield values of SPAD and PEA measurements with no developmental constraints for all *Quercus* species.

Since Chl *a* fluorescence is the light emitted by Chl *a* molecules upon excitation, it could be argued that the Chl concentration has a major influence on the fluorescence yield of a sample. Since SPAD measurements and OJIP transients were recorded from the same leaves within a short time span, correlations across multiple species, seasons, and years were possible. Fig. 6 shows the relationships between fluorescence parameters and SPAD values. For all parameters significant correlations were observed. Similar results have been obtained in different genotypes of *Litchi chinesis* Sonn. (Fu *et al*. 2013), *Carica papaya* L. (Castro *et al.* 2011), and *Coffea canephora* Pierre (Torres-Netto *et al*. 2005). On the contrary, Dinç *et al*. (2012) found only marginal effects of Chl deficiency by magnesium and sulphate starvation on the fluorescence rise kinetics and virtually unchanged F_0 and F_m values in leaves of hydroponically grown sugar beet plants. They concluded that the activity of the remaining electron transport chain remained largely unaffected with no overall changes in the antenna size. In the JIP-test, to quantify the absorption flux per cross section, the cross section is approximated by F_0 and/or F_m ($ABS/CS_0 = F_0$, $ABS/CS_m = F_m$; Strasser and Strasser 1995, Stirbet and Govindjee 2012), assuming a correlation of Chl content with fluorescence intensity. Since data points from the period of leaf development and leaf senescence are present in the correlation analysis of Fig. 6, one could argue that low JIP-test values at low Chl concentrations are not causally dependent, but the product of low photosynthetic capacity during leaf developmental processes. Removing data obtained before 27 July and after 10 September (n = 1497) to include mostly values from the core vegetation time still yielded significant correlations in the above named parameters (not shown). The highest correlation coefficient (R^2 = 0.526, all data, and R^2 = 0.441, n = 1497) in both cases was found in the parameter RC/ABS, a measure of the apparent antenna size [$RC/ABS \sim Chl_{RC}/Chl_{antenna} = Chl_{RC}/(Chl_{tot} - Chl_{RC})$] referring to Chl of PSII only (Stirbet and Govindjee 2011). RC/ABS quantifies the relative amount of fully active

(Q_A reducing) RCs per absorbing antenna Chls (Strasser and Strasser 1995, Stirbet and Govindjee 2011). Since a change in the ratio of PSII to PSI was not assumed due to unaltered ratios of Chl *a* to Chl *b* (Ceppi *et al.* 2012, Holland *et al.* 2014), RC/ABS (as well as F_0 and F_m) may provide a proportional approximation of the total Chl content and correlate with the SPAD value. The correlation was observed, but the coefficients of determination (R^2) were low, due to the large variability of Chl fluorescence parameter values at a given SPAD value, indicating that dependencies are not very strong, at least in higher Chl concentrations. Dinç *et al*. (2012) and Kalaji *et al.* (2014) suggest that changes in F_0 and F_m can be buffered at decreasing Chl content due to a deeper penetration of the light beam and thus a relatively higher fluorescence contribution by Chl molecules situated in lower leaf layers. Stronger changes in fluorescence parameters have to be expected at changing Chl *a*/*b* ratios (Dinç *et al*. 2012), which have only been observed in the advanced phase of senescence. In contrast to F_0, F_m, V_J, V_I, and RC/ABS, the JIP-test parameter PI_{abs} showed a nonlinear relationship to the Chl content due to normalisation operations (*cf.* Fig. 6). For PI_{abs}, high and low values can be expected at high Chl contents whereas at SPAD values below ~ 25 only low values of PI_{abs} were observed. This threshold has also been reported by Percival *et al.* (2008) who observed photosynthetic impairments in leaves of *Q. robur* at SPAD values below 25. Under the natural conditions observed in 2012 and 2013 at the site in Frankfurt, the selected JIP-test parameters were correlated to the leaf Chl content. Different stresses might, however, alter these relationships significantly.

In conclusion, the data provided allow for the first time the classification and ranking of otherwise reference-less SPAD meter and PEA readings, in a continuum of measureable values, observable under naturally occurring seasonal and pronounced stress conditions in *Quercus* species under Central European conditions and the quantification of the buffer range to threshold values, at which severe impediments ought to be expected. The causes for detected decreases in vitality, sensed by the monitoring of functional leaf traits need to be further identified to provide sufficient silvicultural management tools in the restructuring of prone stands by species mixture and species introduction in a proactive climate change mitigation strategy.

References

Abrams M.D.: Adaptations and responses to drought in *Quercus* species of North America. – Tree Physiol. **7**: 227-238, 1990.

Addicott F.T.: Environmental factors in the physiology of abscission. – Plant Physiol. **43**: 1471-1479, 1968.

Balazadeh S., Schildhauer J., Araújo W.L. *et al*.: Reversal of senescence by N resupply to N-starved *Arabidopsis thaliana*: transcriptomic and metabolomic consequences. – J. Exp. Bot. **65**: 3975-3992, 2014.

Barbaroux C., Bréda N.: Contrasting distribution and seasonal dynamics of carbohydrate reserves in stem wood of adult ring-porous sessile oak and diffuse-porous beech trees. – Tree Physiol. **22**: 1201-1210, 2002.

Bauerle W.L., Oren R., Way D.A. *et al*.: Photoperiodic regulation of the seasonal pattern of photosynthetic capacity and the implications for carbon cycling. – P. Natl. Acad. Sci. USA **109**: 8612-8617, 2012.

Björkman O., Demmig B.: Photon yield of O_2 evolution and chlorophyll fluorescence characteristics at 77 K among vascular plants of diverse origins. – Planta **170**: 489-504, 1987.

Both H., Brüggemann W.: Photosynthesis studies on European evergreen and deciduous oaks grown under Central European climate conditions. I. A case study of leaf development and seasonal variation of photosynthetic capacity in *Quercus robur* (L.), *Q. ilex* (L.) and their semideciduous hybrid, *Q.* × *turneri* (Willd.). – Trees **23**: 1081-1090, 2009.

Bussotti F., Pollastrini M., Holland V., Brüggemann W.: Functional traits and adaptive capacity of European forests to climate change. – Environ. Exp. Bot. **111**: 91-113, 2015.

Castro A.A., Pimentel J.D.R., Souza D.S. *et al*.: [Study of preservation of papaya (*Carica papaya* L.) associated with the application of edible films.] – Revista Venezolana de Ciencia y Tecnología de Alimentos **2**: 49-60, 2011. [In Portuguese]

Ceppi M.G., Oukarroum A., Çiçek N. *et al*.: The IP amplitude of the fluorescence rise OJIP is sensitive to changes in the photosystem I content of leaves: a study on plants exposed to magnesium and sulfate deficiencies, drought stress and salt stress. – Physiol. Plantarum **144**: 277-288, 2012.

Christensen J.H., Kanikicharla K.K., Marshall G., Turner J.: Climate phenomena and their relevance for future regional climate change. – In: Climate Change 2013: The Physical Science Basis. Contribution of Working Group I to the Fifth Assessment Report of the Intergovernmental Panel on Climate Change. Pp. 1217-1308. Cambridge University Press, Cambridge-New York 2013.

De Pury D., Farquhar G.D.: Simple scaling of photosynthesis from leaves to canopies without the errors of big-leaf models. – Plant Cell Environ. **20**: 537-557, 1997.

Delpierre N., Dufrêne E., Soudani K. *et al*.: Modelling interannual and spatial variability of leaf senescence for three deciduous tree species in France. – Agr. Forest Meteorol. **149**: 938-948, 2009.

Dinç E., Ceppi M.G., Tóth S.Z. *et al*.: The Chl *a* fluorescence intensity is remarkably insensitive to changes in the chlorophyll content of the leaf as long as the chl *a*/*b* ratio remains unaffected. – BBA-Bioenergetics **1817**: 770-779, 2012.

DWD: [German Climate Atlas, German Meteorological Service.] *Available at*: http://www.dwd.de, 2015. (*Accessed*: 23 February 2015) [In German]

Ellenberg H.: [Vetetation of Central Europe and the Alps.] Pp. 116-135. Verlag Eugen Ulmer, Stuttgart 1996. [In German]

Estrella N., Menzel A.: Responses of leaf colouring in four deciduous tree species to climate and weather in Germany. – Clim. Res. **32**: 253-267, 2006.

Fu X., Zhou L., Huang J. *et al.*: Relating photosynthetic performance to leaf greenness in litchi: A comparison among genotypes. – Sci. Hortic.-Amsterdam **152**: 16-25, 2013.

Grassi G., Magnani F.: Stomatal, mesophyll conductance and biochemical limitations to photosynthesis as affected by drought and leaf ontogeny in ash and oak trees. – Plant Cell Environ. **28**: 834-849, 2005.

Guissé B., Srivastava A., Strasser R.J.: The polyphasic rise of the chlorophyll *a* fluorescence (OKJIP) in heat stressed leaves. – Arch. Sci. Genéve **48**: 147-160, 1995.

Hanewinkel M., Cullmann D.A., Schelhaas M.J. *et al*.: Climate change may cause severe loss in the economic value of European forest land. – Nat. Clim. Change **3**: 203-207, 2013.

Hickler T., Vohland K., Feehan J. *et al*.: Projecting the future distribution of European potential natural vegetation zones with a generalized, tree species-based dynamic vegetation model. – Glob. Ecol. Biogeogr. **21**: 50-63, 2012.

HLUG: [Soilviewer, Hessian Agency for the Environment and Geology.] *Available at*: http://bodenviewer.hessen.de/viewer.htm., 2015. (*Accessed*: 23 February 2015) [In German]

Holland V., Koller S., Brüggemann W.: Insight into the photosynthetic apparatus in evergreen and deciduous European oaks during autumn senescence using OJIP fluorescence transient analysis. – Plant Biol. **16**: 801-808, 2014.

Kalaji H.M., Schansker G., Ladle R.J. *et al*.: Frequently asked questions about *in vivo* chlorophyll fluorescence: practical issues. – Photosynth. Res. **122**: 121-158, 2014.

Körner C., Basler D.: Phenology under global warming. – Science **327**: 1461-1462, 2010.

Kovats R.S.,Valentini R., Bouwer L.M. *et al*.: Europe. – In: Climate Change 2014: Impacts, Adaptation, and Vulnerability. Part B: Regional Aspects. Contribution of Working Group II to the Fifth Assessment Report of the Intergovernmental Panel on Climate. Pp. 1267-1326. Cambridge University Press, Cambridge-New York 2014.

Kreyling J., Stahlmann R., Beierkuhnlein C.: Spatial variation in leaf damage of forest trees after the extreme spring frost event in May 2011. – Allgemeine Forst und Jagdzeitung **183**: 15-22, 2012.

Lacointe A., Kajji A., Daudet F.A. *et al*.: Mobilization of carbon reserves in young walnut trees. – Acta Bot. Gallica **140**: 435-441, 1993.

Larcher W.: [Ecophysiology of plants.] Pp. 237-241. Verlag Eugen Ulmer, Stuttgart 1994. [In German]

Larcher W.: Physiological Plant Ecology: Ecophysiology and Stress Physiology of Functional Groups. Pp. 514. Springer-Verlag, Berlin-Heidelberg 2003.

Menzel A.: Plant phenological anomalies in Germany and their relation to air temperature and NAO. – Climatic Change **57**: 243-263, 2003.

Miersch I., Heise J., Zelmer I., Humbeck K.: Differential degradation of the photosynthetic apparatus during leaf senescence in barley (*Hordeum vulgare* L.). – Plant Biol. **2**: 618-623, 2000.

Miyazawa S.I., Satomi S., Terashima I.: Slow leaf development of evergreen broad-leaved tree species in Japanese warm temperate forests. – Ann. Bot.-London **82**: 859-869, 1998.

Mohammed G.H., Zarco-Tejada P., Miller J.R.: Applications of chlorophyll fluorescence in forestry and ecophysiology. – In: DeEll J.R., Toivonen P.M.A. (ed.): Practical Applications of Chlorophyll Fluorescence in Plant Biology. Pp. 79-124. Springer, Boston 2003.

Morecroft M.D., Stokes V.J., Morison J.I.L.: Seasonal changes in the photosynthetic capacity of canopy oak (*Quercus robur*) leaves: the impact of slow development on annual carbon uptake. – Int. J. Biometeorol. **47**: 221-226, 2003.

Munné-Bosch S., Alegre L.: Die and let live: leaf senescence contributes to plant survival under drought stress. – Funct. Plant Biol. **31**: 203-216, 2004.

Oukarroum A., El Madidi S., Schansker G., Strasser R.J.: Probing the responses of barley cultivars (*Hordeum vulgare* L.) by chlorophyll *a* fluorescence OLKJIP under drought stress and re-watering. –Environ. Exp. Bot. **60**: 438-446, 2007.

Percival G.C., Keary I.P., Noviss K.: The potential of a chlorophyll content SPAD meter to quantify nutrient stress in foliar tissue of sycamore (*Acer pseudoplatanus*), English oak (*Quercus robur*), and European beech (*Fagus sylvatica*). – Arboricult. Urban Forest. **34**: 89-100, 2008.

Petersen R.: [Oak-planting in clusters – first results of a sample area in the forest district Neuhaus.] – Forst und Holz **62**: 19, 2007. [In German]

Schansker G., Tóth S.Z., Strasser R.J.: Methylviologen and dibromothymoquinone treatments of pea leaves reveal the role of photosystem I in the Chl *a* fluorescence rise OJIP. – BBA-Bioenergetics **1706**: 250-261, 2005.

Schär C., Vidale P.L., Lüthi D. *et al*.: The role of increasing temperature variability in European summer heatwaves. – Nature **427**: 332-336, 2004.

Schleip C., Cornelius C., Menzel A.: [When the young shoots of May turn into the young shoots of March.] – LWF Aktuell **85**: 15-18, 2011.

Sparks T.H., Carey P.D.: The responses of species to climate over two centuries: an analysis of the Marsham phenological record, 1736-1947. – J. Ecol. **83**: 321-329, 1995.

Srivastava A., Guissé B., Greppin H., Strasser R.J.: Regulation of antenna structure and electron transport in photosystem II of *Pisum sativum* under elevated temperature probed by the fast polyphasic chlorophyll *a* fluorescence transient: OKJIP. – BBA-Bioenergetics **1320**: 95-106, 1997.

Stirbet A., Govindjee: On the relation between the Kautsky effect (chlorophyll *a* fluorescence induction) and photosystem II: Basics and applications of the OJIP fluorescence transient. – J. Photoch. Photobio. B **104**: 236-257, 2011.

Stirbet A., Govindjee: Chlorophyll *a* fluorescence induction: a personal perspective of the thermal phase, the J-I-P rise. – Photosynth. Res. **113**: 15-61, 2012.

Strasser B.J.: Donor side capacity of photosystem II probed by chlorophyll *a* fluorescence transients. – Photosynth. Res. **52**: 147-155, 1997.

Strasser B.J., Strasser R.J.: Measuring fast fluorescence transients to address environmental questions: The JIP-test. – In: Mathis P. (ed.): Photosynthesis: From Light to Biosphere. Pp. 977-980. Kluwer Academic Publishers, Dordrecht 1995.

Strasser R.J., Tsimilli-Michael M., Qiang S., Goltsev V.: Simultaneous *in vivo* recording of prompt and delayed fluorescence and 820-nm reflection changes during drying and after rehydration of the resurrection plant *Haberlea rhodopensis*. – BBA-Bioenergetics **1797**: 1313-1326, 2010.

Strasser R.J., Tsimilli-Michael M., Srivastava A.: The fluorescence transient as a tool to characterize and screen photosynthetic samples. – In: Yunus M., Pathre U., Mohanty P. (ed.): Probing Photosynthesis: Mechanisms, Regulation and Adaptation. Pp. 443-480. Taylor & Francis, London 2000.

Strasser R.J., Tsimilli-Michael M., Srivastava A.: Analysis of the chlorophyll *a* fluorescence transient. – In: Papageorgiou G.C., Govindjee (ed.): Chlorophyll *a* Fluorescence: A Signature of Photosynthesis. Advances in Photosynthesis and Respiration. Pp. 321-362. Springer, Dordrecht 2004.

Thomas H., Ougham H.: The stay-green trait. – J. Exp. Bot. **65**: 3889-3900, 2014.

Torres-Netto A., Campostrini E., de Oliveira J.G., Bressan-Smith R.E.: Photosynthetic pigments, nitrogen, chlorophyll *a* fluorescence and SPAD-502 readings in coffee leaves. – Sci. Hortic.-Amsterdam **104**: 199-209, 2005.

Wright I.J., Reich P.B., Westoby M. *et al*.: The worldwide leaf economics spectrum. – Nature **428**: 821-827, 2004.

Appendix. JIP-test parameters extracted from the fast Chl *a* fluorescence OKJIP transient. F refers to prompt fluorescence; RC to active (Q_A reducing) reaction centre. According to Strasser *et al.* (2010) and Stirbet and Govindjee (2011).

Data extracted from the recorded fluorescence transient	
F_t	Fluorescence at the time t
$F_{50\mu s}$	First reliable recorded fluorescence at 50μs
$F_{300\mu s} \equiv F_K$	Fluorescence intensity at the K-step (300 μs)
$F_{2ms} \equiv F_J$	Fluorescence intensity at the J-step (2 ms)
$F_{30ms} \equiv F_I$	Fluorescence intensity at the I-step (30 ms)
F_P	Maximal recorded fluorescence intensity at the transient
Fluorescence parameters derived from the extracted data	
$F_0 \equiv F_{50\mu s}$	Minimal fluorescence, when all RCs are open
$F_m (= F_P)$	Maximal fluorescence, when all RCs are closed
$F_v \equiv F_m - F_0$	Maximal variable fluorescence
$V_t \equiv (F_t - F_0)/(F_m - F_0)$	Variable fluorescence at the time t
$\Delta V_{IP} = 1 - V_I$	Relative amplitude of the I-P phase
$V_{OJ300\mu s} = (F_{300\mu s} - F_{50\mu s})/(F_{2ms} - F_{50\mu s})$	Relative amplitude of the K-step
$M_0 \equiv [(\Delta F/\Delta t)_0]/(F_m - F_{50\mu s}) \equiv 4\,(F_{300\mu s} - F_{50\mu s})/(F_m - F_{50\mu s})$	Approximated initial slope (in ms^{-1}) of the fluorescence transient normalized on the maximal variable fluorescence F_v
Biophysical parameters derived from the fluorescence parameters	
$\phi_{Po} \equiv F_v/F_m$	Maximum quantum yield of primary photochemistry/PSII. Efficiency/probability that an absorbed photon leads to a reduction of Q_A
$\psi_{Eo} \equiv 1 - V_J$	Efficiency/probability that an electron moves further than Q_A^-
$\phi_{Do} \equiv 1 - \phi_{Po}$	Efficiency/probability that the energy of an absorbed photon is dissipated as heat
$RC/ABS = \phi_{Po}\,(V_J/M_0)$	Q_A reducing RCs per PSII antenna Chl [reciprocal of ABS/RC = absorption flux (of antenna Chls) per RC (also a measure of PSII apparent antenna size)]
$PI_{abs} \equiv RC/ABS\ \phi_{Po}/(1 - \phi_{Po})\ \psi_{Eo}/(1 - \psi_{Eo})$	Performance index (potential) for energy conservation from photons absorbed by PSII to the reduction of intersystem electron acceptors
OJIP transient normalisations	
Normalised transient F_0 ($= F_{50\mu s}$)	$(F_t)\,(F_{50\mu s})^{-1}$
Double normalised transient $F_{50\mu s}$ & F_m	$(F_t - F_{50\mu s})\,(F_m - F_{50\mu s})^{-1}$
Differential V_{OP} curve	$(F_t^A - F_{50\mu s}{}^A)\,(F_m{}^A - F_{50\mu s}{}^A)^{-1} - (F_t^B - F_{50\mu s}{}^B)\,(F_m{}^B - F_{50\mu s}{}^B)^{-1}$